Theor. Appl. Climatol. 92, 87–101 (2008)
DOI 10.1007/s00704-007-0308-2
Printed in The Netherlands

Theoretical and Applied Climatology

Department of Physics, University of the West Indies, Mona, Jamaica

Toward the development of prediction models for the primary Caribbean dry season

T. S. Stephenson, A. A. Chen, and **M. A. Taylor**

With 5 Figures

Received November 2, 2004; revised November 6, 2006; accepted February 5, 2007
Published online June 27, 2007

Summary

Two statistical models are created for the Caribbean during its dry season. Canonical correlation analysis (CCA) confirms that there is a robust El Niño Southern Oscillation (ENSO) signal in the region during the dry season and that the mode manifests itself as oppositely signed precipitation anomalies over the north and south Caribbean. The south-eastern Caribbean becomes dry in response to a warm event. The first statistical model consequently uses a rainfall index averaged over the south-eastern Caribbean as the predictand. A model which retains an ENSO proxy as one of two predictors shows reasonable skill with hindcast predictions for the region. A second model is created using a Jamaican rainfall index as predictand. Jamaica falls in the transition zone i.e. between the oppositely signed north-south precipitation anomalies characteristic of the ENSO dry season mode. In this case no ENSO related predictor is retained in the final model. Composite analysis of select atmospheric variables for anomalously high and low rainfall years (for the dry season) give an understanding of the dynamics of the Caribbean dry season during phases of the ENSO, particularly those which lead to the creation of the transition zone.

1. Introduction

This study examines the dynamics of the primary Caribbean dry season with the intent to develop models for predicting its rainfall extremes.

The mean climatology of Caribbean rainfall (Fig. 1) indicates a regional wet season from May through October, a primary dry season from November through April, and a secondary but short-lived dry period in late July/early August known as the midsummer drought (Magaña et al., 1999). The seasons are primarily facilitated by the meridional migration of the north Atlantic high pressure cell. During the primary dry season the high pressure system expands equatorward causing lower-tropospheric divergence and subsidence. During the wet season, poleward migration of the high and a northward displaced Pacific Inter-tropical Convergence Zone result in convergence of surface winds and moisture over the Caribbean. There is concomitantly a weakening of both the surface easterlies and upper level westerlies yielding a reduction in vertical shear and favouring convection. A brief equatorward displacement of the high pressure cell in July/early August period facilitates the midsummer drought (Hastenrath, 1976, 1984). Sea surface temperature anomalies (SSTAs) also modulate Caribbean rainfall. For example, tropical north Atlantic SSTAs contribute to *early wet* season rainfall anomalies (Chen et al., 1997; Giannini et al., 2000; Chen and Taylor, 2002; Taylor et al., 2002; Spence et al., 2004), while an east-west SST gradient between the equatorial Pacific and Atlantic modulates the *late wet* season (Giannini et al.,

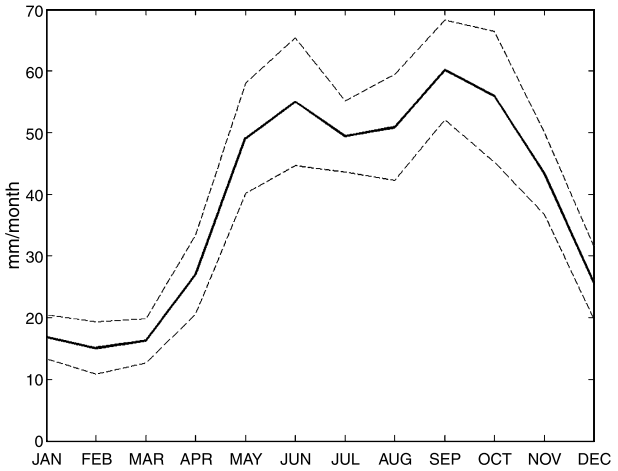

Fig. 1. Mean climatology for the Caribbean rainfall (bold). Standard deviations are also shown (dotted)

2000; Taylor, 1999; Taylor et al., 2002; Spence et al., 2004). A detailed review of the Caribbean dynamics is presented by Ashby et al. (2005).

It is the primary dry season (November–April) which is of interest as (i) the least is known about the drivers of its rainfall anomalies, particularly the role of tropical sea surface temperature anomalies (SSTAs), and (ii) the prevailing dry, cool conditions are important for both the tourism and sugar industries which are major facets of the Caribbean island economies[1]. Enfield and Alfaro (1999), Giannini et al. (2000), Martis et al. (2002) and Spence et al. (2004) suggest that the Caribbean *dry* season exhibits a north-south gradient in rainfall in response to El Niño Southern Oscillation (ENSO) events. When the equatorial Pacific is warm, the north Caribbean is wet and the southern Caribbean is dry, and vice versa (see for example Fig. 3 of Enfield and Alfaro (1999) or Fig. 5 of Spence et al. (2002)). Implied in this pattern is a 'transition zone' from wet to dry which Spence et al. (2004) place along the 17° N latitude line or in the vicinity of Jamaica.

In this paper we first explore the dynamics of the Caribbean dry season as a precursor to developing statistical models for this period. The dynamical analysis addresses questions about the robustness, consistency and the manifestation of the ENSO signal i.e. the viability of the ENSO signal as a basis for dry season models. For example, Enfield and Alfaro (1999) and to a lesser extent Spence et al. (2004) utilize mean dry seasons in their analysis. We utilize canonical correlation analysis (CCA) applied to bi-monthly periods to address whether the signal remains the primary mode of variability throughout the entire season and if its manifestation is consistently a meridional gradient in precipitation. Similarly, Ashby et al. (2005) show that a mean Caribbean precipitation index (10°–20° N and 83°–65° W) captures reasonably well the variability of the region during the wet season, and is therefore a useful predictand. We use the CCA results to determine the viability of the Ashby et al. (2005) index for a dry season statistical model, particularly since it is centered around Jamaica which falls in the dry season's 'transition zone'. We also use composite analysis to examine circulation patterns during anomalously wet or dry Caribbean dry seasons. The composites provide a physical explanation for the ENSO pattern in the Caribbean and justify the choice of some of the predictors for the models to be created.

Section 2 describes the data and methodology used. Sections 3 and 4 outline the results of the CCA and composite analysis respectively. In Sect. 5 we detail model creation and validation. With few exceptions, the development and use of statistical models is in its infancy within the Caribbean region (see Ashby et al., 2005 for a review), and except for the Dutch Caribbean[2] (Martis et al., 2002), none are known to have been attempted for the dry season. Section 6 presents a summary and discussion of the results obtained.

2. Data and methodology

2.1 Data and domain

Caribbean precipitation anomaly data (hereafter PRECIPA) were from the Magaña et al. dataset (Magaña et al., 1999) for the period January 1958–December 1998 from which the climatology was removed. Data are recorded monthly on a $0.5° \times 0.5°$ grid and incorporate station, satellite and model (reanalysis) data. The data were

[1] Dry conditions at this time are necessary for increased sucrose content in sugar cane, while the period coincides with the peak in tourist arrivals.

[2] The ABC islands of the Dutch Caribbean are in general drier than the rest of the Caribbean year round, but experience their wettest months during the Caribbean dry season.

compiled from the archives (i) the National Center for Atmospheric Research (NCAR) for the southern United States, northern South America and the Caribbean Islands, (ii) the Mexican Weather Service, and (iii) the National Weather Services of Central America. These were complemented with microwave sounding unit daily precipitation estimates over the oceans for the period 1979–1996 (Spencer, 1993) and daily reanalysis precipitation estimates over the Intra-American Seas during the pre-satellite era, given the lack of any other source data in this region during this latter period. Validation of the Magaña dataset over the Caribbean and near Caribbean region (7°–25° N, 60°–90° W) is documented by Taylor et al. (2002).

The Reynolds Optimum Interpolated SST dataset (Reynolds, 1988) is also used. The dataset has a $2° \times 2°$ resolution and covers the region 44.5° S–59.5° N and 180° W–180° E. Two smaller SST anomaly datasets are also extracted for the tropical Pacific (180°–80° W; 10° S–30° N) and tropical Atlantic (90°W–0°; 5° S–27° N) oceans. The National Centers for Environmental Prediction (NCEP) $2.5° \times 2.5°$ gridded, monthly, reanalysis dataset (Kalnay et al., 1996) is used to identify the circulation cells present over the Atlantic and Pacific oceans. The domain used spans 20° S–50° N and 170° W–10° E, and the variables examined are the divergent wind, vorticity and pressure vertical velocity. The resolution of the datasets is not sufficient to isolate patterns that are orography-dependent.

2.2 Methodology

Data were aggregated into bi-monthly averages commencing with January–February. Giannini et al. (2000) show that the bi-monthly subdivisions suitably capture the seasonal variability of Caribbean rainfall. Thereafter CCA is employed to isolate temporal and spatial relationships between Pacific and/or Atlantic SSTs and Caribbean precipitation.

CCA decomposes the eigenvector of the cross-correlation matrix between two input variables – in this case between SSTA and PRECIPA – into modes of decreasing explained cross-correlation between the two analyzed fields. Each mode is represented by two singular vectors describing the spatial patterns of weights for the two variables, and two series of expansion coefficients describing the weighting of the mode of the two variables in the temporal domain. Principal component analysis (Kutzbach, 1967; Wallace et al., 1992) is employed as a 'prefilter' to CCA to decrease random sampling fluctuations as a result of the short time series (Bretherton et al., 1992). Principal component analysis allows the original data to be projected onto the leading eigenmodes that account for a large portion of the variance. The eigenmodes are retained using the scree test (Cattell, 1966) and further separated using North's rule (North et al., 1982) so that their sampling errors do not overlap. These modes are then combined separately in CCA.

For each two-month period, CCA is done for PRECIPA and each of the two tropical SSTA datasets. That is, for Jan–Feb, CCA is performed for both PRECIPA and Atlantic SSTA and PRECIPA and Pacific SSTA, and this is repeated for each subsequent two-month period. The ocean basins are separated to observe the consistency/robustness of the SST-rainfall relationships noted in Sect. 1. Diagnostic heterogeneous correlation maps which isolate the spatial patterns associated with a given mode are presented (Wallace et al., 1992; Bretherton et al., 1992). The maps depict the expansion coefficients of one field (e.g. SSTA) correlated with the grid point values of the other field (e.g. PRECIPA). The time coefficients of the SSTA fields for the Pacific and Atlantic are also correlated with SSTA indices defined in Table 1. The correlations help characterize the retained modes and are presented for bi-monthly periods

Table 1. SST indices used in previous studies

Index	Description	Reference
Niño-3	Average for 5° N–5° S and 150°–90° W	Climate Diagnostics Bulletin (2002)
EqA	Average for 5° N–5° S and 0°–15° W	Taylor et al. (2002)
TNA	Average for 6° S–22° N and 60°–15° W	Enfield (1996)
TSA	Average for 22° S–2° N and 35° W–10° E	Enfield (1996)
TNA − TSA	Meridional Gradient SST index	Enfield (1996)
TNA + TSA	Meridional SST index	Enfield and Alfaro (1999)
PacEqA	Zonal Gradient SST index (Niño-3-EqA)	Taylor et al. (2002)

even beyond the dry season so as to judge the relative importance of the SSTA associations in the dry versus the wet season. Statistical significance at the 95% level is assessed using the random phase method (Ebisuzaki, 1997).

Composites are used to examine the *mean* atmospheric circulation for precipitation extremes in the *dry* season. The linear trend is first removed from the CCA mode 1 time coefficients of precipitation for January–February using a triple three-month running mean (Taylor et al., 2002) as we are primarily interested in the seasonal to interannual characteristics of the period. The detrended time series is divided into terciles with the upper and lower terciles representing anomalously high and low precipitation years respectively. The following variables are then composited for high and low years: (i) upper (200 hPa) and lower (850 hPa) level divergent wind anomalies, (ii) upper and lower level vorticity anomalies, (iii) pressure vertical velocity anomalies (VVA) at the medium level (500 hPa), and (iv) VVA for the 1000–200 hPa range.

The compositing technique is after Wang (2002a, b) who suggests the use of both the divergent wind and the vertical velocity to identify atmospheric cells. The divergent component of horizontal wind is represented by the second component in the equation $v = v_\psi + v_\Phi = \mathbf{k}\times\nabla\psi + \nabla\Phi$ where ψ is the stream function and Φ is velocity potential. The first term represents the rotational component which, though the larger term, is not essential for identifying atmospheric cells (Krishnamurti, 1971; Wang, 2002a, b). The pressure vertical velocity (VV) at 500 hPa gives an idea of the mean vertical motion at the mid-tropospheric level, while its profile between the 1000 hPa and 200 hPa levels and averaged over 2.5° S–2.5° N in an east-west plane is used to diagnose motions associated with an east–west circulation along the equator i.e. the Walker circulation cell. Similarly, VV profiles averaged over 60°–40° W and 10° W–10° E in a north-south plane are used to examine meridional cells over the western and eastern Atlantic respectively (Wang, 2002b).

Though similar in approach, the composites of this study differ from those shown in Wang (2002a, b) in that they are with respect to precipitation extremes in the dry season as opposed to extremes in SST and SLP. Domains are also extended to include the western Caribbean. Changes in the large-scale atmospheric circulations are therefore directly related to the Caribbean dry season rainfall pattern which may or may not be related to SST anomalies. Composite difference maps are utilized with regions of significant difference assessed using the Student's *t*-test (Panofsky and Brier 1968; Knaff, 1997).

Finally, statistical models of dry season Caribbean rainfall are created for regions suggested by the CCA analysis. Justification for the regions is offered in Sect. 5. The section also details the choice of predictors and the mechanism for narrowing the predictor pool. The models are created using two multiple linear regression (MLR) approaches. The first employs backward elimination (BE) where predictor variables that fail a partial *F*-test at the alpha significance level of 0.05 are eliminated. In the second, a stepwise procedure is used and Akaike Information Criteria (AIC) weights are assigned to model parameters. Variables contributing the least information at each step are eliminated (Akaike, 1973, 1974, 1983). The final model is one that yields the lowest AIC value.

The models are validated using the cross-validation method (Hastenrath, 1995; Drosdowsky and Chambers, 2001) for the 1958–1995 period and using independent data for 1996–2003. The following skill scores are used in assessing the regression models:

(i) The model skill (S): Correlation between the forecast and observed values.
(ii) The coefficient of determination (R^2): The percentage of variation in the observed data accounted for by the regression line
(iii) The multiple R: The square root of the R^2.

The regression models are further evaluated by categorical scores for three categories: Very Wet, Average, and Very Dry. Additional assessment scores include:

(iv) The Hit Rate (HR): The percentage of perfect categorical forecasts.
(v) The Skill Score (SS): A variation of the HR, where SS has a chance value of zero, a score of +100% for a set of perfect hits and −100% for a set of forecasts with no hits.
(vi) The Linear Error in Probability Space (LEPS) Score: A measure of how close

the forecast and observed values are in terms of the probability density function of the observations (Ward and Folland, 1991; Potts et al., 1996). LEPS penalizes a forecast that is two categories in error more than another which is only one category in error.

(vii) The Probability of Detection (POD) above or below normal: The percentage of correct above or below normal events predicted.

(viii) The False Alarm Rate (FAR) above or below normal: The percentage of far above or below forecast which failed to materialize.

All the scores are consistent with those detailed in Alfaro (2000) and Ashby et al. (2005). A perfect model would have SS, LEPS, and PODs of 100% and FARs of zero. A good model would have positive SS and LEPS, PODs greater than 50% and FARs less than 33.3%.

3. CCA results

3.1 CCA statistics

The three leading Pacific and Atlantic SSTA modes from principal component analysis prefiltering explain 75–86% and 68–76%, respectively of each basin's variability, while the first three PRECIPA modes explain 49–63% of the observed rainfall variability. It is the first three principal component analysis modes in each case which are combined and used in the CCA.

The leading CCA modes of Pacific (P1) and Atlantic (A1) variability for each 2-month period account for 13–25% and 14–22%, respectively of the bi-monthly precipitation variability and exhibit modest (0.52) to robust (0.84) correlations with the primary PRECIPA mode. These values are higher than that explained by the second CCA modes in all bimonthly periods except for July–August for the Pacific. Subsequent discussions are therefore confined to the primary modes.

3.2 Pacific SSTA variability and Caribbean precipitation

Table 2 shows the correlations between the time coefficients of Pacific SSTA (P1) and PRECIPA (PR1) for the first CCA mode and the SSTA indices of Table 1. P1 shows significant and robust correlations with both the niño-3 and EqA indices for the Caribbean dry season i.e. November through April. EqA and niño-3 indices are however significantly correlated (>0.90) for the same months and P1 is therefore deemed an ENSO mode. (See Giannini et al., 2000 for a discussion of the strong association between the equatorial Pacific and equatorial Atlantic during boreal winter of ENSO years). Significant correlations between the leading PRECIPA mode (PR1) and the niño-3 index (Table 2b) also confirm the sig-

Table 2. Correlations of primary CCA modes of (**a**) Pacific SSTA and (**b**) PRECIPA and SSTA indices. Indices are as defined in Table 1. Values in bold are significant at the 95% level

Indices	Jan–Feb	Mar–Apr	May–Jun	Jul–Aug	Sep–Oct	Nov–Dec
a						
Niño-3	**−0.91**	**−0.87**	−0.08	**−0.66**	**−0.66**	**−0.81**
TNA	**−0.42**	**−0.43**	−0.20	0.38	**−0.69**	−0.37
TSA	**−0.48**	−0.34	**−0.60**	**0.47**	**−0.59**	**−0.59**
TNA − TSA	0.06	−0.10	0.33	−0.20	0.11	0.30
TNA + TSA	**−0.61**	**−0.54**	**−0.56**	**0.50**	**−0.73**	**−0.59**
EqA	**−0.93**	**−0.84**	−0.29	−0.29	**−0.81**	**−0.87**
PacEqA	**−0.85**	**−0.77**	0.03	**−0.75**	**−0.56**	**−0.75**
b						
Niño-3	**−0.65**	**0.72**	0.10	**−0.58**	**0.39**	**−0.57**
TNA	−0.28	**0.37**	−0.29	0.36	**0.62**	−0.01
TSA	−0.37	0.16	0.35	0.13	0.30	−0.37
TNA − TSA	0.08	0.17	**−0.47**	0.15	0.16	**0.36**
TNA + TSA	**−0.45**	**0.38**	0.06	0.27	0.50	−0.25
EqA	**−0.67**	**0.71**	0.15	−0.35	**0.48**	**−0.62**
PacEqA	**−0.60**	**0.64**	0.07	**−0.62**	**0.33**	**−0.52**

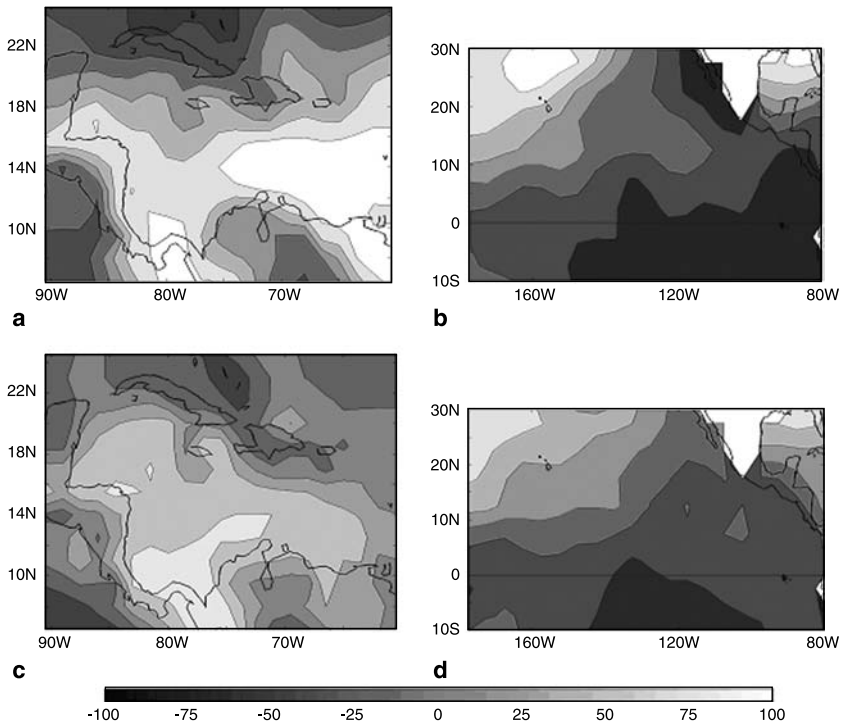

Fig. 2. CCA results for PRECIPA and Pacific SSTA for January–February (**a**–**b**) and November–December (**c**–**d**). Panels (**a**) and (**c**) show the distribution of scalar correlation (shading and contour interval is 0.2×100) between the gridded PRECIPA and mode 1 expansion coefficients for Pacific SSTA. Panels (**b**) and (**d**) show the distribution of scalar correlation between the gridded Pacific SSTA and mode 1 expansion coefficients for PRECIPA. The average 95% significance levels are 0.31 and 0.35, respectively

nificance of the ENSO-Caribbean rainfall relationship for the dry season.

The Jan–Feb heterogeneous maps (Fig. 2a, b) illustrate the pattern of the association. Equatorial Pacific SSTAs are negatively correlated with precipitation anomalies in the southern Caribbean basin (south of approximately 18° N and centered on the south-eastern Caribbean islands) and positively correlated with anomalies to the north, and vice versa. It is a warm (cold) equatorial Pacific which is associated with negative (positive) rainfall anomalies over the southern Caribbean and positive (negative) rainfall anomalies in the north, particularly over Cuba and southern Florida. A transition zone between the oppositely signed precipitation anomalies is established between 18° and 20° N and encompasses Jamaica, Hispaniola and Puerto Rico. There are no significant correlations in this zone. Figure 2a is consistent with the ENSO-related precipitation pattern for the Caribbean and Central American region during boreal winter (Enfield and Alfaro, 1999; Giannini et al., 2000; Spence et al., 2004).

We note that the ENSO associated north-south precipitation gradient is still present in March–April (not shown), though regions of significant correlation are confined to the Leeward Islands (12°–14° N; 62°–65° W) in the south and to the far north Caribbean above 24° N. By May–June however (i.e. the early rainfall season) the equatorial Pacific influence disappears and (as seen from Table 2) the strongest significant correlations for P1 and PR1 are with tropical Atlantic indices (TSA, TNA + TSA and TNA − TSA, respectively). During the remainder of the wet season (July–August and September–October) inter basin zonal SSTA gradients and the tropical Atlantic become significant (see also Taylor et al., 2002). By November–December however the ENSO signal is once again robust (see Table 2) and a basin of oppositely signed precipitation anomalies in the northern and southern Caribbean is again apparent (Fig. 2c, d).

3.3 Atlantic variability and Caribbean precipitation

The correlations between the leading Atlantic and Pacific SSTA modes (A1 vs. P1) and between their corresponding precipitation modes (AR1 vs. PR1) were calculated (not shown). P1 correlates significantly with A1 in all bi-monthly periods, with strongest correlations during the Caribbean dry season and in particular from January through April (−0.93 and −0.95). Low-

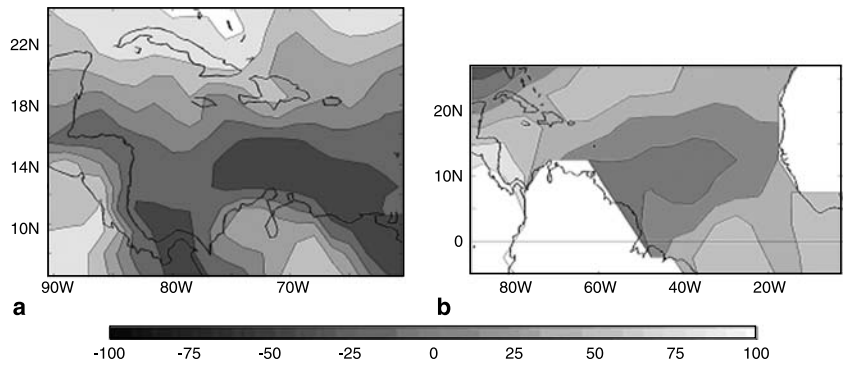

Fig. 3. As in Fig. 2 but for CCA of PRECIPA and Atlantic SSTA

est correlation between the two primary SSTA CCA modes is during May–June (0.49).

A1 is considered a proxy of Pacific variability in the dry season, i.e. two winter ENSO modes are effectively obtained in spite of our separation of the Atlantic and Pacific basins. This would explain the high correlations between A1 and P1 and is likely due to the inclusion of a small portion of the eastern equatorial Pacific in the Atlantic SSTA domain (see Fig. 3b). It nonetheless underscores the dominance of the equatorial Pacific in the dry season over tropical Atlantic influences. We contrast this, for example, with the Caribbean in May–June during which a north–south tropical Atlantic SSTA gradient emerges as the primary Atlantic mode (not shown) in spite of the inclusion of the equatorial Pacific in the Atlantic SSTA domain.

There is therefore (not surprisingly) a strong similarity between the A1 heterogeneous SST on precipitation map obtained for Jan–Feb (Fig. 3a) and that shown in Fig. 2a for the first Pacific CCA mode. The oppositely signed north-south Caribbean precipitation signal is evident in the first winter Atlantic mode. Note also the significant correlation with the eastern equatorial Atlantic as would also be anticipated from Table 2.

In tandem the CCA analysis of both Pacific and Atlantic basins suggest the ENSO signal is robust and strong during the Caribbean dry season even more so than for other periods throughout the year. ENSO indices or their proxies are good potential predictors of rainfall anomalies for the period. The signal is also consistent in its manifestation and the CCA maps indicate the south-eastern Caribbean as a region where an ENSO-based model would likely be effective. We discuss this further in Sect. 5.

4. Composites

We examine the mean atmospheric circulation for years when the Caribbean dry season exhibits rainfall extremes. Since the January–February interval is at the height of the dry period it is taken as representative of the entire period, and the detrended time series of its first CCA precipitation mode is used to determine high and low rainfall years (see again Sect. 2). Composites were made for precipitation and the other previously noted atmospheric variables using the Magaña and reanalysis datasets, respectively.

High (low) precipitation years correspond to a wet (dry) south-eastern and dry (wet) north Caribbean (see again Fig. 2a). It is of significance that even though the composites were done on the basis of rainfall extremes, 9 of the 14 low rainfall years were El Niño years while 4 of the 8 high rainfall years correspond to La Niña years. This further confirms the robustness of the ENSO signal during this period. Not surprisingly, the regions of significant precipitation difference between high and low years (not shown) replicates Fig. 2a, though Puerto Rico no longer falls within the transition zone.

The corresponding mean atmospheric circulation is gleaned from Fig. 4a–e. Figure 4a, b show two areas of statistically significant difference between high and low years for anomalous low and upper level divergence, located in the equatorial and north Pacific Ocean. The patterns imply anomalous low (upper) level divergence (convergence) over the equatorial Pacific during high years, as would be the case during cold equatorial Pacific episodes. From similar regions of significance difference in the Atlantic we infer that anomalous low (upper) level convergence

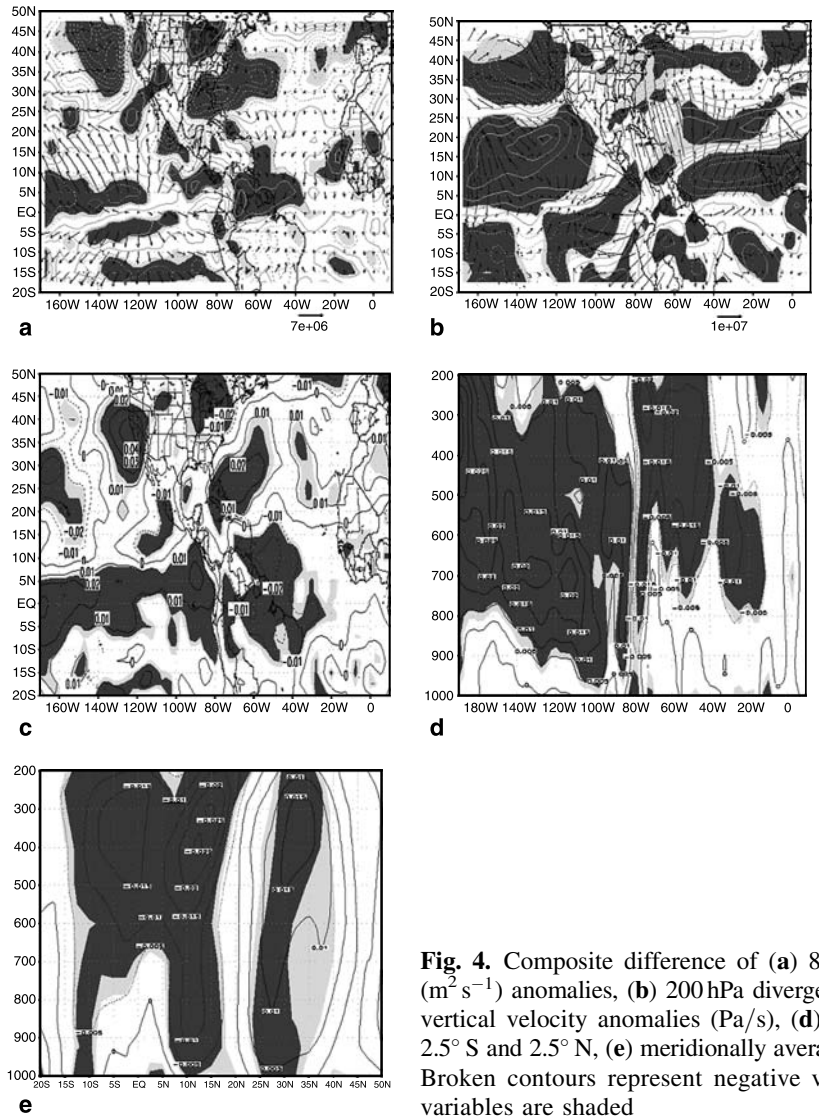

Fig. 4. Composite difference of (**a**) 850 hPa divergent wind (ms^{-1}) and vorticity ($m^2\,s^{-1}$) anomalies, (**b**) 200 hPa divergent wind and vorticity anomalies, (**c**) 500 hPa vertical velocity anomalies (Pa/s), (**d**) zonally averaged vertical velocity between 2.5° S and 2.5° N, (**e**) meridionally averaged vertical velocity between 60° and 40° W. Broken contours represent negative values. Significant differences in contoured variables are shaded

(divergence) exists over the Amazon and western equatorial Atlantic and anomalous low (upper) level divergence (convergence) over Florida and the tropical north Atlantic during high years. The areas of significant divergence anomalies are accompanied by changes in cyclonic and anticyclonic motion as indicated by the changes in vorticity. The patterns of Fig. 4a and b are reminiscent of the Pacific North American (PNA) pattern (Wallace and Gutzler, 1981; Horel and Wallace, 1981) and clearly show its influence penetrating the northern Caribbean during the dry season.

From Fig. 4c regions of significant change in the 500 hPa vertical velocity exist over the equatorial and north Pacific with anomalous medium level descent implied for high years. Recall that vertical motions at midlevel are a useful indicator of coupling between the upper and lower troposphere. By comparison, anomalous descent exists over the northern Caribbean and tropical north Atlantic while anomalous ascent occurs over the Amazon and western equatorial Atlantic.

Difference composites of upper and lower level zonal and meridional wind anomalies (not shown) complete the circulation picture. The patterns reveal that low level westerlies and upper level easterlies dominate east of the equatorial Pacific low-level divergent centre and extend across Central and South America and into the Caribbean during high years. Significant changes in upper and lower level meridional wind anomalies also occur in the Atlantic between 0° and 20° N and extend from the Caribbean to the western

coast of Africa. Over this region it is anomalous low level northerlies and upper level southerlies that exist during high years.

The resulting picture is that during high years when the south-eastern (north) Caribbean is wet (dry) there is an anomalous Walker cell characterized by ascent over the Amazon and the south-eastern Caribbean, easterly flow aloft, descent over the equatorial eastern Pacific and low level westerly flow back to the Amazon. Figure 4d shows the anomalous ascent (descent) throughout the troposphere over the Amazon and western equatorial Atlantic (eastern equatorial Pacific). This anomalous circulation pattern would yield the positive rainfall anomalies over the south-eastern Caribbean. There is also an anomalous Hadley cell involving anomalous ascent over the Amazon coupled with anomalous descent at approximately 25°–35° N (Fig. 4e). The latter region of descent penetrates the northern Caribbean, resulting in the anomalous drying over this area. A reversal of the anomalous Walker and Hadley cells occurs for low years yielding in the negative (positive) precipitation anomalies over the south-eastern (north) Caribbean.

The composite analysis also suggests that Jamaica and Hispaniola are situated at the edge of the anomalous ascending limb of the Hadley to the immediate south and the anomalous descending limb to the immediate north. This cancels the impact of ENSO induced anomalies in these circulations on the islands of this region. This explains the lack of any significant correlations in Fig. 2b in this region or any significant difference in precipitation between high and low years (not shown). It is unlikely that any model for Jamaica or its vicinity would incorporate ENSO as a predictor in spite of its robust signal during the dry season.

5. Statistical models

5.1 Predictors and predictands

The heterogeneous precipitation maps (Figs. 2a, c and 3a) eliminate the possibility of using the Caribbean rainfall index of Taylor et al. (2002) or Ashby et al. (2005) as the predictand for the dry season. Unlike for the wet season, it is not representative of the principal mode of variability across the basin. A statistical model is instead attempted for an index centered on the south-eastern Caribbean where the ENSO impact is strong (Figs. 2a, 3a). The south-eastern Caribbean anomalous rainfall index (SCI) was constructed from the Magaña et al. dataset and is an area average over the domain 12°–16° N, 60°–65° W over January and February for the period 1958–1995. SCI correlates significantly with rainfall stations on islands within or just outside the domain (e.g. Dominica – 0.69, Barbados – 0.68, Anguilla – 0.82 and Montserrat – 0.55)[3].

For comparison we also attempt a model for Jamaica (18° N, 77° W) which was consistently located in the 'transition zone'. A Jamaica anomalous rainfall index (JI) was constructed by averaging data over January and February for 1958–1995 obtained from 43 stations across the island. JI correlates significantly (0.98) with a 180-station index used by Hall (2003) and with data obtained for Jamaica from the Climatic Research Unit (CRU) time series (TS) 2.0 gridded dataset (Mitchell et al., 2002, 2003) (0.99).

Table 3 shows the predictors used to create the SCI and JI models respectively. The predictors were culled from a much larger predictor pool which was not restricted to SST indices but included (i) a full suite of global indices (e.g. Niño-1,2,3 and 4, the North Atlantic Oscillation index, the Atlantic Warm Pool index, the Quasi-biennial Oscillation, etc.), (ii) area averaged indices representing regions of strong correlation up to one year's lag as deduced from correlation maps between the predictands and selected atmospheric variables (not shown), and (iii) indices specially constructed to capture the atmospheric dynamics discussed in the previous section. The predictors retained in Table 3 were those which showed significant correlations with the two predictands. SO and ND as referenced in the table represent the September–October and November–December periods, respectively.

Note from Table 3 that there are separate predictor pools for SCI and JI thereby justifying the decision to create separate models. There are four SCI predictors (Niño-3, SOI, PNA and SLPZN) which capture the strong ENSO modulation of rainfall over the south-eastern Caribbean

[3] Station data for a number of Caribbean islands were obtained from the Caribbean Institute for Meteorology and Hydrology (CIMH) located in Barbados.

Table 3. List of potential predictors for the (**a**) SCI and (**b**) JI. SO and ND represent the September–October and November–December periods respectively

	Predictors	Bi-monthly divisions	Description	Correlations
a				
1	Niño-3	SO	As defined in Table 2.1	−0.58
2	SOI	SO	As defined in Table 2.1	0.58
3	PNA	SO	As defined in Table 2.1	−0.38
4	SLPZN	SO	Difference of SLPA averaged over 25°–30° S, 120°–130° W and 0°–5° N, 0°–10° W	0.74
5	SH	ND	Specific humidity anomalies averaged over 12.5°–15° N, 92.5°–95° W–700 hPa level	−0.56
6	ZW2	SO	Zonal wind anomalies averaged over 17.5°–20° N, 87.5°–90° W–200 hPa level	−0.67
b				
1	SLPZSUM	SO	[SLPA(2.5° N-2.5° S, 135°–140° W)–SLPA(5°–10° S, 40°–45° W)] + [SLPA(37.5°–42.5° N, 60°–65° W) –SLPA (35°–40° N, 30°–35° W)]	0.61
2	SST	ND	SSTA averaged over 35.5°–40.5° N, 29.5°–39.5° W	−0.52
3	SHMER	SO	Difference of Specific humidity anomalies averaged over 25° E–27.5° N, 85°–90° W and 15°–17.5° N, 80°–82.5° W–700 hPa level	0.58
4	ZWDIF	ND	Difference of 200 hPa and 850 zonal wind anomalies averaged over 7.5°–10° N, 72.5°–77.5° W	0.44

during the dry season. In addition, the ZW2 variable is taken as representative of the influence of the atmospheric circulation anomalies, while SH it is believed illustrates the more regional influences on rainfall variability. Note also that there are no Pacific SSTA predictors for Jamaica. Instead the JI predictors comprise SLPZUM and SHMER which capture meridional gradients in pressure and moisture between regions north and south of the transition zone. The North Atlantic SST index we believe is a proxy for the influence of the NAH, while ZWDIF captures zonal atmospheric circulation anomalies over the northern South American.

5.2 The South-eastern Caribbean model

Models were created and validated using the techniques outlined in Sect. 2. In the first instance SCI models using only the Niño-3 index were created. Only that for BE is shown below as the skill was almost identical irrespective of the

Table 4. Cross-validation assessments of the regression models for predicting the SCI and JI. S is the skill; R^2 is the coefficient of determination; R is the multiple correlation coefficient; HR is the Hit Rate; SS is the Skill Score; LEPS is the Linear Estimation in Probability Space; FARBN and FARAN are the false alarm scores for below normal and above normal forecast; PODBN and PODAN are the probability scores for predicting below normal and above normal events

	South-eastern Caribbean		Jamaica	
Model Predictors	Niño-3(SO)	SLPZN(SO), ZW2(SO)	SHMER(SO), ZWDIF(ND), SST(ND)	SHMER(SO), ZWDIF(ND), SST(ND), SLPZSUM(SO)
S	0.53	0.80	0.84	0.82
R^2	0.32	0.69	0.71	0.72
R	0.57	0.83	0.84	0.85
HR	0.73	0.81	0.84	0.78
SS	0.59	0.72	0.76	0.68
LEPS	0.43	0.64	0.69	0.57
FARBN	0.25	0	0	0.08
FARAN	0	0	0	0
PODBN	0.75	0.67	0.67	0.67
PODAN	0.46	0.77	0.85	0.69

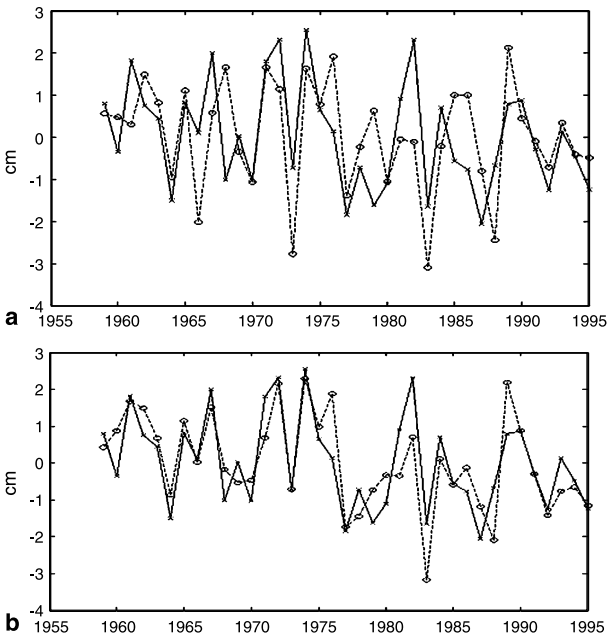

Fig. 5. Plot of forecasted versus observed monthly rainfall anomalies for south-eastern Caribbean. Forecasted values obtained using the (**a**) Niño-3(SO) predictor, and (**b**) SLPZN(SO) and ZW2(SO) predictors. Dashed lines and circles represent forecasted values

technique applied. $\widehat{Y}_{SCI}$ is the forecasted value of the SCI, that is, the average rainfall amount over January and February in centimetres. The SCI model's skill is assessed by the scores given in column 1 of Table 4 and by the plot of forecast versus observed values shown in Fig. 5a.

$$\widehat{Y}_{SCI-BE} = 0.0189 - 0.6925\,\text{Niño(SO)}$$

A model with Niño-3 alone does reasonably well at predicting the variability of the south-eastern Caribbean over the hindcast period as indicated by Fig. 5a and the assessment scores. The model has a R^2 value of 32% and a SS of 0.59.

If we do not constrain ourselves to the Niño-3 predictor but include the other significantly correlated variables of Table 3, models of better skill emerge. The models now obtained for the SCI from BE and AIC are:

$$\widehat{Y}_{SCI-BE} = 0.0967 + 0.0353\ \text{SLPZN(SO)} - 0.2533\ \text{ZW2(SO)}$$

$$\widehat{Y}_{SCI-AIC} = 0.0971 + 0.0352\ \text{SLPZN(SO)} - 0.2535\ \text{ZW2(SO)}$$

The units of SLPZN(SO) and ZW(SO) are gpm and ms^{-1} respectively. Note that even though the SCI model does not retain the niño-3 index explicitly, it does retain SLPZN(SO) which correlates significantly with both the niño-3 (0.71) and SOI (0.76) indices i.e. it retains the equatorial Pacific influence.

Column 2 of Table 4 provides an indication of the skill of these SCI models as does Fig. 5b. The value of R^2 is 0.69 and the skill score is 0.72. HR, which is an indicator of the ability of the model to predict very wet, average and very dry conditions is 81%. The PODAN and PODBN values of 77% and 67%, respectively and the false alarm rates of zero for above and below normal events further imply that these SCI regression models exhibit reasonable skill in forecasting extreme events during the Caribbean dry season.

The models' abilities were further tested using independent data compiled from four islands in the south-eastern Caribbean – Barbados, Dominica, St. Vincent and Grenada. Rainfall data for the

Table 5. Same as Table 4 but using the independent data for the period 1996–2003 for anomalous rainfall over the south-eastern Caribbean and Jamaica

	South-eastern Caribbean	Jamaica	
Model Predictors	SLPZN(SO), ZW2(SO)	SHMER(SO), ZWDIF(ND), SST(ND)	SHMER(SO), ZWDIF(ND), SST(ND), SLPZSUM(SO)
S	0.48	0.47	0.46
R^2	0.53	0.52	0.74
R	0.73	0.72	0.86
HR	0.63	0.44	0.78
SS	0.44	0.17	0.67
LEPS	0.23	−0.23	0.62
FARBN	0	0.67	0
FARAN	0	0.50	0.25
PODBN	0.50	0.33	0.67
PODAN	0.33	0.25	0.75

period 1996–2003 were obtained for one station in each of the four islands. Rainfall anomalies were computed and the data averaged to obtain an anomalous south-eastern Caribbean rainfall index. The SLPZN(SO) and ZW2(SO) predictors were obtained from the NCEP/NCAR NCAR reanalysis data available from the NOAA-CIRES Climate Diagnostics Center web site at http://www.cdc.noaa.gov/. The predictors were used to generate a timeseries of predicted rainfall anomalies which was compared to the observed anomalous rainfall index. The models skill scores are summarized in Table 5.

The SLPZN(SO) and ZW2(SO) predictors explain 53% of variability for the period and exhibit a hit rate of 63% and a probability of detection of above and below normal precipitation of 33 and 50%, respectively. The models also demonstrate a false alarm rate of zero for above and below normal rainfall events again suggesting a fair degree of skill. We anticipate that the estimates of model skill would have been even greater if the Magaña dataset used to train and cross-validate the models over the 1958–1995 period, was also available for 1999–2003.

5.3 The Jamaica model

The models obtained for JI are given by:

$$\begin{aligned}\widehat{\mathbf{Y}}_{\mathrm{JI-BE}} = &-0.0021 + 2.5127\ \mathrm{SHMER(SO)} \\ &+ 0.0004\ \mathrm{ZWDIF(ND)} \\ &- 0.0019\ \mathrm{SST(ND)}\end{aligned}$$

$$\begin{aligned}\widehat{\mathbf{Y}}_{\mathrm{JI-AIC}} = &-0.00160 + 2.19480\ \mathrm{SHMER(SO)} \\ &+ 0.00031\ \mathrm{ZWDIF(ND)} \\ &- 0.00108\ \mathrm{SST(ND)} \\ &+ 0.00003\ \mathrm{SLZSUM(SO)}\end{aligned}$$

$\widehat{\mathbf{Y}}_{\mathrm{JI}}$ is the forecasted value of the JI in cm. The units of SHMER, ZWDIF, SST and SLPZSUM are kg/kg, ms^{-1}, °C and gpm, respectively. The coefficients of both equations are to the order 10^3. Using the AIC technique SLPZSUM(SO) is retained as an additional predictor. The JI models capture approximately 72% of the January–February rainfall variability for Jamaica and exhibit a HR of 78 and 84% (Table 4). The main difference between the BE and AIC models is with the PODAN, as the BE model has a value of 85 vs. 69% for the AIC model.

Skill tests performed on station data for Jamaica for the period 1996–2003 reveal that the model with all four predictors [SHMER(SO), ZWDIF(ND), SST(ND) and SLPZSUM(SO)] exhibits greater skill than the model comprising only three predictors (c.f. Table 5). The four-predictors model has a hit rate of approximately 78%, PODBN and PODAN of 67 and 75%, respectively and false alarm rate above normal and below normal of 0 and 25% respectively. This is in comparison to an HR of 44%, PODBN and PODAN of 33 and 25%, respectively and FARBN and FARAN of 67% and 50% respectively exhibited by the three-predictor model.

6. Discussion and summary

Our aim was to investigate the possibility of creating statistical models for dry season rainfall in the Caribbean. We used CCA to first confirm that ENSO is the dominant mode of rainfall variability for the Caribbean dry season and that the mode manifests itself as oppositely signed precipitation anomalies over the northern Caribbean (north of approximately 20° N) and southern Caribbean. The ENSO signal is strong over the far northern and the south-eastern Caribbean with the latter (former) being negative (positive) during a warm Pacific event. A transition zone from positive to negative rainfall anomalies (or vice versa) occurs in the 18°–20° N latitudinal band and includes Jamaica, Hispaniola and Puerto Rico, where ENSO impact appears to be non-existent.

The findings put in context the results of other sub-regional studies which report increased winter rainfall over Florida and Cuba in relation to warm ENSO events (Schmidt et al., 2001; Naranjo-Diaz, 2001, respectively), decreased rainfall over the Dutch Caribbean (Martis et al., 2002), and an absence of ENSO-related precipitation over Puerto Rico (Malmgren et al., 1998). The results also extend the work of Enfield and Alfaro (1999), Giannini et al. (2000), and Spence et al. (2004) by showing that the signal and its corresponding gradient rainfall pattern is a robust feature of the *entire* dry period. CCA results for other bi-monthly periods confirm a fading of the ENSO signal by May–June which is consistent with the findings of Giannini et al. (2000) and Taylor et al. (2002).

Composite analysis sheds light on the dynamics governing the observed SSTA-rainfall

relationships or lack of it in the transition zone. The pattern of an anomalously wet south-eastern Caribbean and dry north Caribbean seemingly results from anomalous Walker and Hadley cells over the Pacific and Atlantic sectors. The anomalous Walker (Hadley) cell involves air ascending over the Amazon, western equatorial Atlantic and south-eastern Caribbean, diverging to the west (north), descending over the eastern equatorial Pacific (tropical-subtropical Atlantic), and returning toward the east (south). The ascent over the Amazon and western equatorial Atlantic yields the positive rainfall anomalies over the south-eastern Caribbean. The descent over the tropical Atlantic penetrates the northern Caribbean region yielding the anomalous drying in this region. We propose that the anomalous circulation cells are linked to the ENSO phenomenon, thereby making the results consistent with the findings of Wang (2002a), but extrapolated westward to include the Caribbean. This westward extrapolation allows us to further hypothesize that it is the coincidence of the ascending and descending limbs of the anomalous Hadley cell which leads to a cancellation of the ENSO effect over that region of the Caribbean deemed the 'transition zone'.

We further note that the circulation anomalies presented are consistent with a northward displacement of both the Atlantic equatorial trough and the north Atlantic high from their climatological positions during boreal winter of a La Nina event and vice versa (Hastenrath and Heller, 1977). Converse conditions during an El Niño i.e. a weakening of the equatorial trough and North Atlantic High, would indeed yield an anomalously dry south-eastern and wet northern Caribbean. The weakening of the high pressure system occurs in tandem with an equatorial displacement of the midlatitude jet stream (in turn a spin-off of the warm ENSO induced PNA pattern). This results in increased penetration of polar fronts into the south-eastern United States and Gulf of Mexico (Ropelewski and Halpert, 1986, 1989; Kiladis and Diaz, 1989) and by extension the northern Caribbean sector.

Finally, there is evidence of predictability of dry season rainfall anomalies over the *south-eastern* Caribbean on the basis of the strong ENSO modulation of rainfall in this region. It is important to note that the single Caribbean rainfall index utilized in other modeling studies as representative of the region's variability is not applicable for the dry season. For the south-eastern Caribbean, the model with greatest skill retains two predictors. They are a zonal SLP gradient over the equatorial Pacific and Atlantic (the Pacific having the stronger loading) and an index representing 200 hPa zonal wind strength over the Central American region. Both offer predictability two months prior to the start of the dry season, i.e. September–October. However since the zonal gradient is considered a proxy for the ENSO influence, and an ENSO model shows reasonable skill, the lead time for prediction may be a little longer as ENSO events are predictable up to a few additional months prior to onset (Goddard et al., 2001).

There is also evidence of the predictability of dry season rainfall for Jamaica which is situated within the transition zone, though with completely different predictors. Not surprisingly, no ENSO indices or their proxies are retained for the Jamaican model. Instead the predictors of Jamaican rainfall include: (i) a meridional gradient in specific humidity over the Caribbean, (ii) a sum of zonal SLP gradients situated over the equatorial Pacific and Atlantic and over the Atlantic midlatitudes for September–October, (iii) north Atlantic SST and (iv) a difference in upper and lower level winds over the northern South America for November–December. Three of the four predictors highlight the importance of gradients in atmospheric parameters in determining the predictability of rainfall over Jamaica and by extension the transition zone. The dynamics of the transition zone are however not well understood and need to be further investigated.

Future work would therefore involve the use of a dynamical regional model to further examine the circulation features of the dry season, as well as an investigation of inter-ENSO variability (Kumar and Hoerling, 1997; Hoerling and Kumar, 1997; Hoerling et al., 1997) during the Caribbean dry season rainfall.

Acknowledgement

This research is partially funded by the Inter-American Institute for Global Change Research (IAI) initiatives PESCA 5, CRN 73 (Victor Magaña, PI) and CRN 48 (Ulisses Confalonieri, PI). We thank Albert Owino for his insight that shaped some of the concepts in this paper. Special thanks to the Caribbean Institute for Meteorology and Hydrology

for making available data for some south-eastern Caribbean islands and to the Canefield Airport in Dominica for its assistance in acquiring data for Dominica.

References

Akaike H (1973) Information theory and an extension of the maximum likelihood principle. Second Int Symp on Information Theory. Akademia Kiado, Budapest, Hungary: pp 267–281

Akaike H (1974) A new look at the statistical model identification. IEEE Trans Automat Contr AC-19: 716–723

Akaike H (1983) Information measures and model selection. Bull Int Statistical Institute 50: 277–290

Alfaro E (2000) Response of air surface temperatures over Central America to Oceanic Climate Variability Indices. Tópicos Meteorológicos y Oceanográficos 7(2): 63–72

Ashby SA, Taylor MA, Chen AA (2005) Statistical models for predicting Caribbean rainfall. Theor Appl Climatol 82: 65–80; DOI 10.1007/s00704-004-0118-8

Bretherton CS, Smith C, Wallace JM (1992) An Intercomparison of methods for finding coupled patterns in climate data. J Climate 5: 541–560

Cattell RB (1966) The scree test for the number of factors. Multivar Behav Res 1: 245–276

Chen AA, Taylor MA (2002) Investigating the link between early season Caribbean rainfall and the El Niño + 1 year. Int J Climatol 22: 87–106

Chen AA, Roy A, McTavish J, Taylor M, Marx L (1997) Using SST Anomalies to predict flood and drought conditions for the Caribbean. COLA Technical report No. 49, 24

Drosdowsky W, Chambers LE (2001) Near-global sea surface temperature anomalies as predictors of Australian rainfall. J Climate 14: 1677–1687

Ebisuzaki W (1997) A method to estimate the statistical significance of a correlation when the data are serially correlated. J Climate 10: 2147–2153

Enfield DB, Alfaro EJ (1999) The dependence of Caribbean rainfall on the interaction of the tropical Atlantic and Pacific Oceans. J Climate 12: 2093–2103

Giannini A, Kushnir Y, Cane MA (2000) Interannual variability of Caribbean rainfall, ENSO and the Atlantic Ocean. J Climate 13: 297–311

Goddard L, et al (2001) Current approaches to seasonal-to-interannual climate predictions. Int J Climatol 21: 1111–1152

Hall T (2003) Relationships between Jamaican September, October and November Rainfall and hurricane predicting parameters. M. Phil. Thesis, University of The West Indies, Mona, 23 pp

Hastenrath S (1976) Variations in low-latitude circulation and extreme climatic events in the tropical Americas. J Atmos Sci 33: 202–215

Hastenrath S (1984) Interannual variability and the annual cycle: mechanisms of circulation and climate in the tropical Atlantic sector. Mon Wea Rev 112: 1097–1107

Hastenrath S (1995) Recent advances in tropical climate prediction. J Climate 8: 1519–1533

Hastenrath S, Heller L (1977) Dynamics of climatic hazards in northeast Brazil. Quart J Roy Meteor Soc 103: 77–92

Hoerling MP, Kumar A (1997) Why do North American climate anomalies differ from one El Niño event to another? Geophys Res Lett 24: 1059–1062

Hoerling MP, Kumar A, Zhong M (1997) El Niño, La Niña and the nonlinearity of their teleconnections. J Climate 10: 1769–1786

Horel JD, Wallace JM (1981) Planetary-scale atmospheric phenomena associated with the Southern Oscillation. Mon Wea Rev 109: 813–829

Kalnay E, Kanmitsu M, Kistler R, et al (1996) The NCEP/NCAR 40-year reanalysis project. Bull Amer Meteor Soc 77: 3437–3471

Kiladis GN, Diaz HF (1989) Global climatic anomalies associated with extremes in the southern oscillation. J Climate 2: 1069–1090

Knaff JA (1997) Implications of summertime sea level pressure anomalies in the Tropical Atlantic Region. J Climate 10: 789–804

Krishnamurti TN (1971) Tropical east–west circulations during the northern summer. J Atmos Sci 28: 1342–1347

Kumar A, Hoerling MP (1997) Interpretation and Implications of the Observed Inter-El Niño variability. J Climate 10: 83–91

Kutzbach JE (1967) Emperical eigenvectors of sea-level pressure, surface temperature and precipitation complexes over North America. J Appl Meteor 6: 791–802

Magaña V, Amador JA, Medina S (1999) The midsummer drought over Mexico and Central America. J Climate 12: 1577–1588

Malmgren BA, Winter A, Chen D (1998) El Niño-Southern Oscillation and North Atlantic Oscillation control of climate in Puerto Rico. J Climate 11: 2713–2717

Martis A, van Oldenborgh GJ, Burgers G (2002) Predicting rainfall in the Dutch Caribbean – more than El Niño? Int J Climatol 22: 1219–1234

Mitchell TD, Hulme M, New M (2002) Climate data for political areas. Area 34: 109–112

Mitchell TD, Carter TR, Jones PD, Hulme, New M (2003) A comprehensive set of high-resolution grids of monthly climate for Europe and the globe: the observed record (1901–2000) and 16 scenarios (2001–2100). J Climate (submitted)

Naranjo-Diaz L (2001) Cuba country case study: Impacts and responses to the 1997–98 El Niño event. In: Glantz NH (ed) Once burned, twice shy: lessons learned from 1997–98 El Niño. Tokyo, Japan: The United Nations University, pp 67–77

North GR, Bell TL, Cahalan F, Moeng FJ (1982) Sampling errors in the estimation of empirical orthogonal functions. Mon Wea Rev 110: 699–706

Panofsky HA, Brier G (1968) Some applications of statistics to meteorology. Pennsylvania: The Pennsylvania State University, 224 pp

Potts JM, Folland CK, Jolliffe I, Sexton D (1996) Revised "LEPS" scores for assessing climate model simulations and long-range forecasts. J Climate 9: 34–53

Reynolds RW (1988) A real time global sea surface temperature analysis. J Climate 1: 75–86

Ropelewski CF, Halpert MS (1986) North American precipitation and temperature patterns associated with the El Niño/Southern Oscillation (ENSO). Mon Wea Rev 114: 2352–2362

Ropelewski CF, Halpert MS (1989) Precipitation patterns associated with the high index phase of the southern oscillation. J Climate 2: 268–284

Schmidt N, Lipp EK, Rose JB, Luther ME (2001) ENSO influence on seasonal rainfall and river discharge in Florida. J Climate 14: 615–628

Spence JM (2002) Examining the effect of concurrent sea surface temperature anomalies on Caribbean rainfall. M. Phil. Thesis, University of The West Indies, Mona, 73 pp

Spence JM, Taylor MA, Chen AA, et al (2004) The effect of concurrent sea surface temperature anomalies in the tropical Pacific and Atlantic on Caribbean Rainfall. Int J Climatol 24: 1531–1541; DOI: 10.1002/joc.1068

Spencer RW (1993) Global oceanic precipitation from MSU during 1979–1991 and comparisons to other climatologies. J Climate 6: 1301–1326

Taylor MA (1999) October in May: the effect of tropical Atlantic SSTs on early season Caribbean rainfall. Ph.D. thesis, University of Maryland, College Park, 213 pp

Taylor MA, Enfield DB, Chen AA (2002) The influence of the tropical Atlantic vs. the tropical Pacific on Caribbean Rainfall. J Geophys Res 107(C9): 3127; DOI: 10.1029/2001/JC001097

Wallace JM, Gutzler DS (1981) Teleconnections in the geopotential height field during the Northern Hemisphere winter. Mon Wea Rev 109: 784–812

Wallace JM, Smith C, Bretherton CS (1992) Singular value decomposition of wintertime sea surface temperature and 500-mb height anomalies. J Climate 5: 561–576

Wang C (2002a) Atmospheric circulation cells associated with the El Niño Southern Oscillation. J Climate 15: 399–419

Wang C (2002b) Atlantic climate variability and its associated atmospheric circulation cells. J Climate 15: 1516–1536

Ward MN, Folland CK (1991) Prediction of seasonal rainfall in the North Nordeste of Brazil using eigenvectors of sea surface temperature. Int J Climatol 11: 711–743

Authors' address: Tannecia S. Stephenson (e-mail: tannysyd@yahoo.com), A. Anthony Chen (e-mail: anthony.chen@uwimona.edu.jm), Michael A. Taylor (e-mail: michael.taylor@uwimona.edu.jm), Department of Physics, University of the West Indies, Mona, Jamaica.